UNIVERSITÀ DEGLI STUDI DI CATANIA

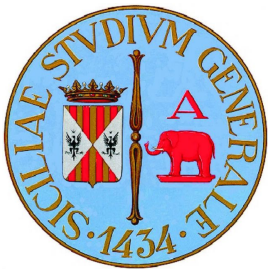

Dipartimento di Fisica é Astronomia

Doctor of Philosphy
Cycle XXXI
Physics

$K^{*}(892)^{\pm}$resonance with ALICE detector at LHC

Candidate:
Kunal GARG

Coordinator:
Prof. Francesco Riggi

Supervisor:
Dr. Angela Badala

In conclusion, it appears to me that nothing can be more improving to a young naturalist, than a journey in distant countries. It both sharpens, and partly allays that want and craving, which, as Sir J. Herschel remarks, a man experiences although every corporeal sense be fully satisfied. The excitement from the novelty of objects, and the chance of success, stimulate him to increased activity. Moreover, as a number of isolated facts soon become uninteresting, the habit of comparison leads to generalization. On the other hand, as the traveller stays but a short time in each place, his descriptions must generally consist of mere sketches, instead of detailed observations. Hence arises, as I have found to my cost, a constant tendency to fill up the wide gaps of knowledge, by inaccurate and superficial hypotheses.

But I have too deeply enjoyed the voyage, not to recommend any naturalist, although he must not expect to be so fortunate in his companions as I have been, to take all chances, and to start, on travels by land if possible, if otherwise, on a long voyage. He may feel assured, he will meet with no difficulties or dangers, excepting in rare cases, nearly so bad as he beforehand anticipates. In a moral point of view, the effect ought to be, to teach him good-humoured patience, freedom from selfishness, the habit of acting for himself, and of making the best of every occurrence. In short, he ought to partake of the characteristic qualities of most sailors. Travelling ought also to teach him distrust; but at the same time he will discover, how many truly kind-hearted people there are, with whom he never before had, or ever again will have any further communication, who yet are ready to offer him the most disinterested assistance.

The Voyage of the Beagle, Charles Darwin

CONTENTS

LIST OF FIGURES

LIST OF TABLES

INTRODUCTION

The present thesis is the result of my Ph.D. research programme as member of the ALICE Collaboration at the CERN (European Organization for Nuclear Research) laboratories. The main interest of this high energy physics experiment is connected to the study *strong nuclear* force which is one of the four fundamental interaction forces. On the nuclear dimension scale (1-3 fm) this is the force that binds protons and neutrons (nucleons) together to form the nuclei of an atom; on a even smaller scale (less than about 0.8 fm, the radius of a nucleon), it is the force that holds quarks together to form protons, neutrons and other particles, all called hadrons.

ALICE experiment is designed to probe the characteristics of the nuclear matter phase diagram. **Quantum Chromodynamics** (QCD) predicts the existence of a state of matter called *Quark-Gluon Plasma* (QGP), which consists of asymptotically free strong-interacting quarks and gluons, which are ordinarily confined by colour confinement inside atomic nuclei or other hadrons at extremely high temperatures and densities. This is the state of matter that is believed to have existed in the early stages of the evolution of our universe. We can recreate QGP in high energy collisions involving ions and protons. *maybe an image of phase diagram*

In addition, the study of the so called nuclear modification factor as a function of transverse momentum (p_T) and the study of multi-strange baryon production in pp collisions can give insight into their production mechanism. In particular, the large transverse momentum range covered by the identification techniques adopted in the ALICE experiment provides the possibility of studying the competition between the hard mechanism (fragmentation) and soft mechanism (coalescence) in the different p_T regions.

This thesis is divided in seven chapters.

chapter 1 The general physics context, with an introduction to QCD and the connection with the idea of the QGP, obtained at high density and temperature, is given in this first chapter. In addition a general description of the fundamental characteristics of heavy-ion collision and the time evolution of the created system are presented.

chapter 2 This chapter is focused on the theoretical description of the strangeness production mechanisms (within the thermodynamical description) and the original idea of strangeness enhancement. Furthermore, results on the nuclear modification factor and the strangeness enhancement obtained in lower energy experiments are shown.

chapter 2 In this chapter the detection capabilities of the ALICE apparatus are given. Moreover, the details on the different steps necessary to convert the electronic signals from the detectors into data suitable for analysis are presented.

chapter 3 Here, the identification technique, based on the topological reconstruction of the weak decay of the multi-strange baryons, is described. Details on the difference between the two systems produced during the collision in Pb–Pb and pp are discussed.

chapters 4 and 5 In these two chapters all the needed steps to measure the production rates of multi-strange baryons, in Pb–Pb and pp collisions respectively, are detailed.

chapter 6 In this last chapter the physical results are presented. Transverse momentum spectra are first compared to model predictions. Then, results on the strangeness enhancement and the nuclear modification factors for the multi-strange baryons at the LHC energy are presented and discussed.

1 PHYSICS OF THE QUARK-GLUON PLASMA

2 | STRANGENESS PRODUCTION IN A QUARK-GLUON PLASMA

2.1 large hadron collider

The Large Hadron Collider (LHC) is the world's largest and most powerful particle accelerator. It first started up on 10 September 2008, and consists of a 27-kilometre ring of superconducting magnets with a number of accelerating structures to boost the energy of the particles along the way. The LHC has a circumference of 27 km. By design, its maximum achievable energies are 7 TeV for beam of protons and 2.76 TeV per nucleon for beam of lead ions, thus providing collisions at $\sqrt{s}$ = 14 TeV and $\sqrt{s_{NN}}$ = 5.5 TeV, respectively. These would be the largest energies ever achieved in particle collision experiments.

Inside the accelerator, two high-energy particle beams travel at close to the speed of light before they are made to collide. The beams travel in opposite directions in separate beam pipes - two tubes kept at ultrahigh vacuum. They are guided around the accelerator ring by a strong magnetic field maintained by superconducting electromagnets. The accelerator has to bend the beams around the ring, keep the bunches focused and accelerate them to their collision energy. Finally, the spatial dimension of the bunches has to be minimised in order to attain high luminosity, which ensure a high number of collisions per time interval at the collision points, i.e. a high luminosity[1]. A combination of magnetic and electric field components performs the mentioned tasks. Despite the high luminosity reached, only a very small fraction of the particles of two bunches collides in a single bunch crossing. The others leave the interaction region essentially uninfluenced, are defocused, and continue to circulate in the accelerator.

Injection of bunches into the LHC (Figure 1) is preceded by acceleration in the LINAC2, PS booster, PS, and SPS accelerators. The acceleration sequence is slightly different for heavy-ions, in which case bunches pass the LINAC3, LEIR, PS, and SPS accelerators (more information can be found in [**?**]). Several injections to the LHC are needed until all bunches of both beams are filled.

1 For a particle accelerator experiment, the luminosity is defined by: $\mathcal{L} = fnN^2/A$ with n number of bunches in both beams, N number of particles per bunch, cross-sectional area A of the beams that overlap completely, and revolution frequency f. The frequency of interactions (or in general of a given process) can be calculated from the corresponding cross-section σ and the luminosity: $dN/dt = \mathcal{L}\sigma$.

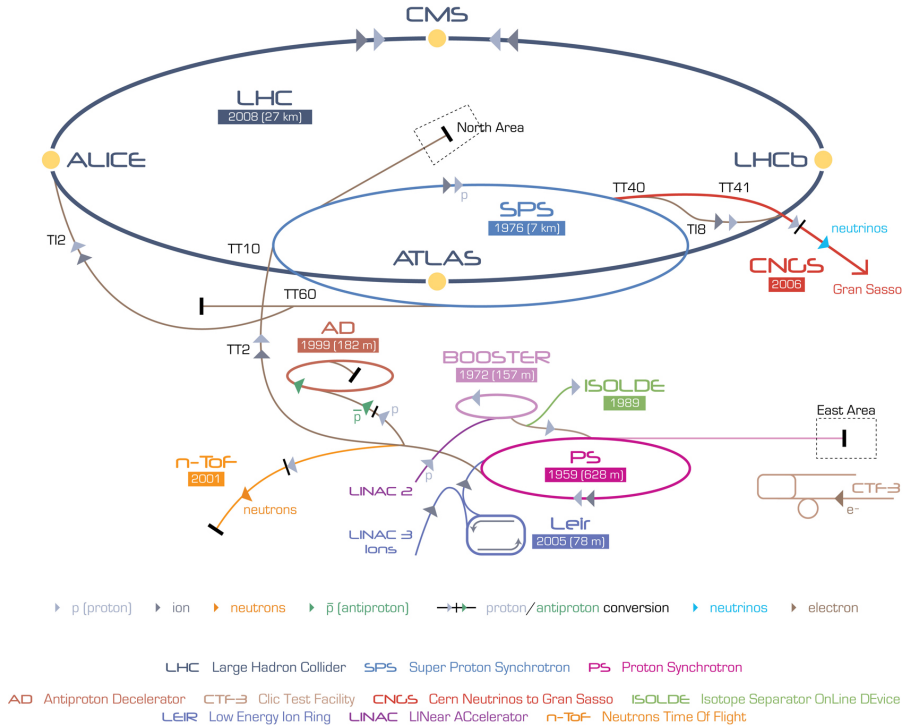

Figure 1: The CERN accelerator complex. [**?**]

3 MEASUREMENT OF K^{*0} PRODUCTION IN PP COLLISIONS

Short lived resonances are good probes to study the properties of strongly interacting matter produced in high energy heavy ion collisions. K^{*0} is a resonance particle with a small lifetime ($\sim$ 4 fm/c), comparable to that of the fireball which is produced during the heavy ion collision. Due to its short lifetime, it can be used to study the re-scattering and regeneration effects. K^{*0} can provide the information regarding strangeness enhancement as it contains a strange quark. Measurements of K^{*0} in pp collisions can be used as a baseline to study the Pb–Pb collisions at the LHC energy and to provide a reference for tuning event generators. Study on $K^{*0}$was done to learn the analysis procedures. In this way, an already available result could be used as a benchmark to test the method followed in the analysis.

I shall describe the measurement of K^{*0} mesons produced at mid-rapidity ($|y| \leqslant 0.5$) in minimum-bias pp collisions at $\sqrt{s}$ = 13 TeV. In this analysis, K^{*0} has been reconstructed by its hadronic decay channel $K^{*0} \rightarrow K^{\pm} + \pi^{\mp}$. The yield of K^{*0} is extracted from 1K invariant-mass distributions as a function of transverse momentum. The p_T spectrum is integrated to obtain a measurement of the total dN/dy, and the mean transverse momentum $\langle p_T \rangle$ is extracted from the spectrum.

3.1 k^{*0}reconstruction in pp collisions

The K^{*0} production in pp collisions at $\sqrt{s}$ = 13 TeV has been done with data collected in 2015 by ALICE detector. The analysis strategy is based on the invariant mass study of reconstructed pairs whose origin could be the decay of K^{*0} mesons into charged particles. The daughter particles are identified as oppositely charged pions and kaons among the tracks reconstructed in the central barrel. Track selection and particle

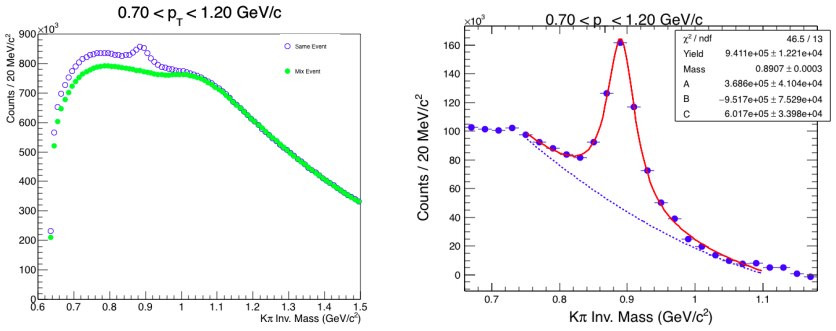

Figure 2: (Left) Unlike-sign invariant mass distribution (open blue circles) and invariant mass obtained by mixed events (green circles) for transverse momentum range $0.7 - 1.20$ GeV/c. The distribution obtained by event mixing technique is normalised in the range $1.1 - 1.3$ GeV/c^2. (Right) Unlike-sign invariant mass distribution after background subtraction for the transverse momentum range $0.7 - 1.2$ GeV/c. Red curve represents the result of the fit. Blue dashed curve represents the background estimated by a polynomial.

identification is described further in this chapter. To extract the yields of K^{*0} mesons in each p_T bin, the invariant-mass distribution of unlike-charge pairs from the same event is computed. The combinatorial background is estimated by event-mixing technique and subtracted from the unlike-charge distribution. In event-mixing technique, the combinatorial background is constructed through the invariant mass of pions and kaons of different events having similar z-vertex, and multiplicity. The mixed event is normalised by the same event distribution in the region of invariant mass of 1.1 to 1.3 GeV/c^2. The signal is obtained by subtracting the mixed event combinatorial background from the same event kaon - pion invariant mass distribution. (see Figure 2)

The p_T dependent correction due to the detector acceptance and reconstruction efficiency, (eff = Acc x ϵ_{rec})(p_T), is computed using Monte Carlo simulations that describes at relative per cent level the detector geometry and response. ϵ_{rec} in particular contains the contribution of tracking and candidates selection cuts. Raw counts are also corrected for the decay branching ratio (BR) and final yield is estimated using:

$$\frac{d^2N}{dp_T dy} = \frac{\text{Raw Counts}}{N_{MB} \times BR \times dp_T \times dy \times \text{eff}} \times f_{norm} \times f_{SL} \qquad (1)$$

where factor $f_{norm} = 0.852^{+0.062}_{-0.03}$ is efficiency for trigger selection for inelastic pp collisions. The factor $f_{SL} = 0.931264$

accounts for the signal loss introduced by the requirement that a primary vertex must be reconstructed and be in the range of ± 10 cm.

3.2 data sample and event selection

The data used for this analysis was taken during June 2015 pp run (LHC15f, pass 2 reconstruction [1]). The full sample consists of 104 runs totalling to about 527×10^6 events. Out of these, only 48 runs have been used, which are marked by the collaboration as 'good runs' i.e. they are characterized by good performance of the detectors and good running conditions (e.g. low level of beam induced background). In particular, all these "good runs" have both the TPC and all the ITS sub-detectors turned on.

The purpose of the event selection is to select hadronic interactions with the highest possible efficiency, while rejecting the machine-induced and physical backgrounds. The ALICE online minimum bias (MB) trigger for this pp run was configured to require the following two conditions:

(i) a signal above the threshold in V0A,

(ii) a signal above the threshold in V0C.

The threshold in the VZERO detector corresponds approximately to the energy deposition of a minimum ionizing particle.

For this analysis, a sample of 45×10^6 minimum bias pp events has been processed where ITS, TPC and TOF performance was optimal. Out of this, around 16 million events satisfy the following selection criteria and have been actually used for the analysis:

- Is InComplete DAQ check.
- Pileup Rejection using AliAnalysisUtils::IsPileUpEvent().
- SPD Clusters vs. Tracklets Check using AliAnalysisUtils::IsSPDClusterVsTrackletBG with default parameters.

1 A few reconstruction processes are needed to obtain data usable for physics analysis. Usually the first two reconstruction passes (pass 0 and pass 1) are needed for quality assurance check and calibration of the main detectors. The pass 2 is the first usable reconstruction for analysis purpose. Further passes are needed to implement signals from detectors requiring special calibrations.

– Event has a track or SPD primary vertex identified.

– SPD vertex-z resolution < 0.25 cm.

– SPD vertex dispersion < 0.04 cm.

– z-position difference between track and SPD vertex < 0.5 cm.

– vertex-z position : $|v_z| < 10$ cm.

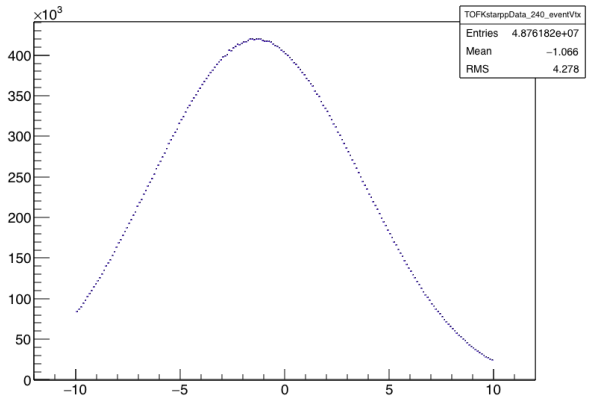

Figure 3: Vertex z coordinate distribution of the accepted events.

The distribution of vertex z position of the accepted events is reported in Figure 3. Events with $|V_z| < 10$ cm have been used to ensure a uniform acceptance in the central pseudorapidity region, $|h| < 0.8$, where the analysis is performed.

3.2.1 Track Selection

The K^{*0} is studied by reconstructing its hadronic decay into charged particles $K^{\pm}\pi^{\mp}$ (B.R. = 66.6%). Because of its very short lifetime of $\sim 4 fm/c$, the resonance decays early after its production and does not make it out of the beampipe. The selection of the candidate daughters is a challenge for the K^{*0} reconstruction, because the produced kaon and pion and undistinguishable from the charged primary particles produced in the "bulk". The candidate resonance daughters with $p_T > 0.15$ GeV/c in the pseudorapidity interval $|h| < 0.8$, are first of all selected by applying cuts on the quality of the reconstruction, related to:

– Reject kink daughters.

– Minimum number of rows crossed in TPC is 70.

- TPC χ^2 clusters < 4.0
- ITS χ^2 clusters < 36.0
- $|DCA|_z < 2$ cm
- $(DCA)_r < 0.0105 + 0.0350 p_T^{-1.01}$
- Pair rapidity $< |0.5|$

The cuts listed above define the "standard quality cuts".

3.2.2 Particle Identification

The daughter particles of $K^{*0}$are charged kaons and pions and they can be identified by using Time Projection Chamber (TPC) and Time Of Flight (TOF) detectors. Particle identification in TPC is performed by measuring the specific energy loss (dE/dx) in the detector gas. The energy loss is described by the Bethe-Bloch function:

$$\langle \frac{dE}{dx} \rangle = \frac{4\pi N e^4}{mc^2} \frac{Z^2}{\beta^2} \Big(\ln \frac{2mc^2\beta^2\gamma^2}{I} - \beta^2 - \frac{\delta(\beta)}{2} \Big) , \qquad (2)$$

where mc^2 is the rest energy of the electron, Z the charge of the projectile, N the number density of electrons in the traversed matter, e the elementary charge, β the velocity of the projectile and I is the mean excitation energy of the atom. A truncated mean that rejects the 40% largest cluster charges is built, resulting in a Gaussian dE/dx response. The measured energy loss is compared to standard energy loss (Bethe-Bloch function) for different particles to identify them. The dE/dx resolution ranges between $5-8\%$ depending on the track inclination angle and drift distance, the energy loss itself and the centrality of the collisions due to the different detectors.

The TOF detector is based on Multigap Resistive Plate Chamber technology. It measures the time of flight of particles with an intrinsic resolution of $\sim$ 80 ps. The expected flight time for each particle species is calculated during the reconstruction, and then PID is performed via a comparison between the measured and expected times. Both pions and kaons are selected by a cut of $|N\sigma_{TPC}| < 2.0$ with a TOF veto of $|N\sigma_{TOF}| < 3.0$. TOF veto means that the TOF cut is applied only for cases where the track matches a hit in the TOF. (see Figure 4 and Figure 5)

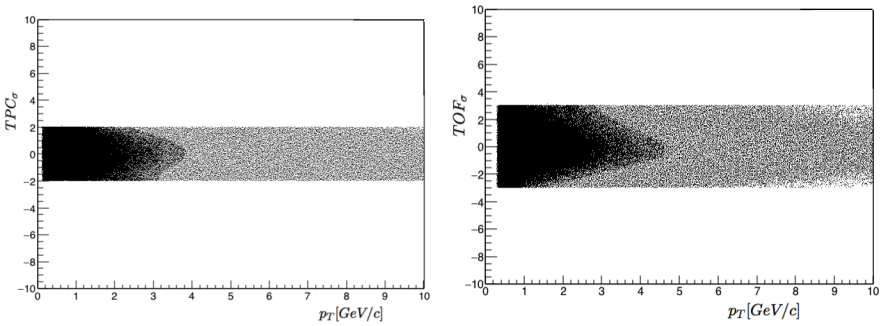

Figure 4: (Left) TPC sigma for π vs p_T. (Right) TOF sigma for π vs p_T

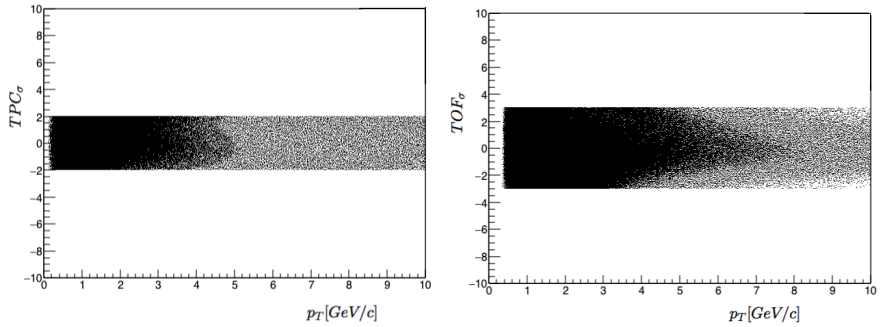

Figure 5: (Left) TPC sigma for K vs p_T. (Right) TOF sigma for K vs p_T

3.3 signal extraction using event mixing

To extract the yields of K^{*0} mesons in each p_T bin, the following procedure is used. The invariant-mass distribution of unlike-charge pairs from the same event is computed. The combinatorial background is estimated by event-mixing technique and subtracted from the unlike-charge distribution.

In event-mixing technique, the combinatorial background is constructed through the invariant mass of pions and kaons of different events having similar z-vertex, and multiplicity. For the reconstruction, we mix 5 events which have z-vertex difference within 1 cm and multiplicity difference within 5. The mixed event is normalised by the same event distribution in the region of invariant mass of 1.1 to 1.3 GeV/c^2. (see Figure 6) The signal is obtained by subtracting the mixed event combinatorial background from the same event kaon - pion invariant mass distribution. (see Figure 6)

After subtraction of combinatorial background, a certain amount of background is left under the K^{*0} signal, which is known as residual background. The source of this residual background may be:
1. correlated real $K\pi$ pairs from other resonance decay.
2. correlated but misidentified $K\pi$ pairs.
The invariant mass calculated from misidentified pairs can not be subtracted away by mixed event background and it remains as a residual background.

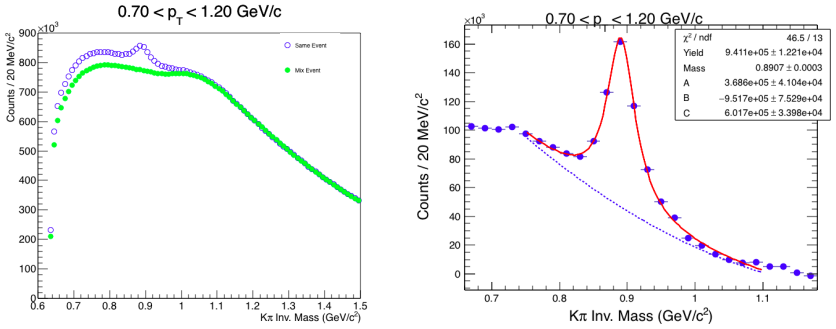

Figure 6: (Left) Unlike-sign invariant mass distribution (open blue circles) and invariant mass obtained by mixed events (green circles) for transverse momentum range $0.7 - 1.20$ GeV/c. The distribution obtained by event mixing technique is normalised in the range $1.1 - 1.3$ GeV/c^2. (Right) Unlike-sign invariant mass distribution after background subtraction for the transverse momentum range $0.7 - 1.2$ GeV/c. Red curve represents the result of the fit (see text). Blue dashed curve represents the background estimated by a polynomial (see text)

3.4 mass

The background-subtracted unlike-charge invariant mass distribution is fitted by a function given by the sum of a non-relativistic Breit-Wigner function and a second order polynomial.

$$\frac{Y}{2\pi}\frac{\Gamma_0}{(M_{K\pi}-M_0)^2+\frac{\Gamma_0^2}{4}} + \text{Polynomial}$$

where M_0 and Γ_0 are the mass and width of the K^{*0}, $M_{K\pi}$ is $K\pi$ invariant mass. The parameter Y gives the Breit-Wigner area. The mass values obtained for the different p_T bin are reported in Figure 7.

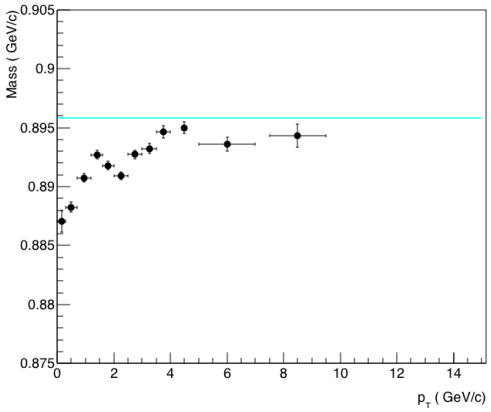

Figure 7: Mass vs. p_T. The line represent the $K^*(892)^o$ PDG mass value.

3.5 raw yield extraction

K^{*o} raw yield for each p_T bin is obtained by fitting the invariant mass distribution while fixing the width value to the PDG one (0.0474 GeV/c^2). The raw yield is obtained from the Y parameters of the Breit-Wigner function.
The yield has been estimated in 13 p_T bins lying between : 0, 0.3, 0.7, 1.2, 1.6, 2.0, 2.5, 3.0, 3.5, 4.0, 5.0, 7.0, 10.0, 15.0 GeV/c. The invariant mass distributions and the fit results for the different p_T bins are shown in Figure 8.

The raw yield p_T spectrum is shown in Figure 9.

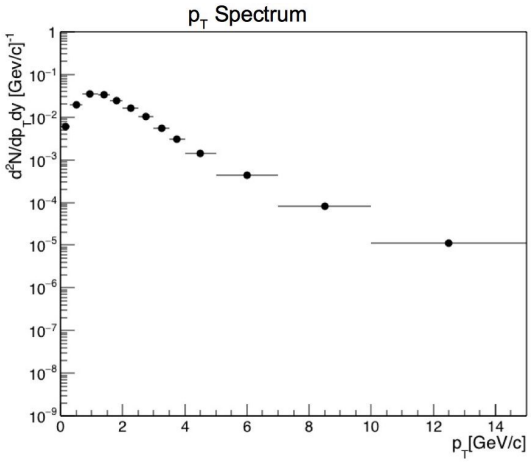

Figure 9: K^{*o} raw yield spectrum.

3.6 monte carlo

3.6.1 Efficiency x acceptance of K^{*0}

Acceptance is defined as the percentage of generated particles whose final states are geometrically included in the detector. Efficiency takes into account detector limitations that for a given particle depend on the mass, charge, momentum etc.

We use Monte Carlo productions to estimate our efficiency x acceptance. In our present case, we used the Monte Carlo production LHC15g3a3 which was generated using PYHTIA8 - Monash 2013. PYTHIA is an example of event generators which are software libraries that generate simulated high-energy particle physics events. In most processes a factorisation of the full process into individual problems is possible, these individual processes are calculated separately, and the probabilistic branching between them is performed using Monte Carlo methods. The final-state particles generated by event generator is fed into the detector simulation, allowing a precise prediction and verification for the entire system of experimental setup.

The acceptance times efficiency is defined as the ratio of the number of reconstructed K^{*0} mesons having decay daughters ($K^{\pm}\pi^{\mp}$) that passes through the track cuts which are used in real data analysis to the number of generated K^{*0} with same decay daughter in rapidity interval ± 0.5.

$$\epsilon_{rec} = \frac{N_{reconstructed}}{N_{generated}}$$

The uncertainty in ϵ_{rec} is calculated using the Bayesian approach. The choice of bayesian approach is motivated by the fact that the events of numerator and denominator are correlated. The standard deviation for the efficiency $\epsilon_{rec} = k/n$, where the numerator k is a subset of the denominator n, is:

$$\sigma_{\epsilon} = \sqrt{\frac{k+1}{n+2}\left(\frac{k+2}{n+3} - \frac{k+1}{n+2}\right)}$$

The K^{*0} acceptance x efficiency distribution as a function of p_T is shown in Figure 10.

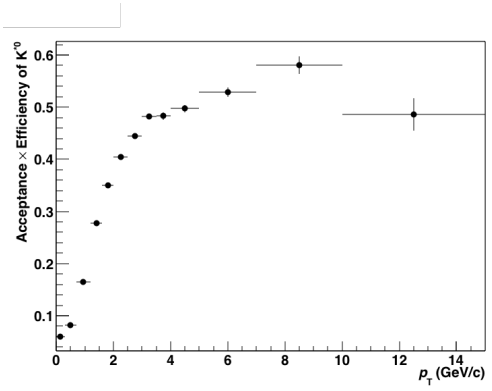

Figure 10: Efficiency x Acceptance vs p_T for K^{*o}

3.6.2 Corrected p_T spectrum

To extract the yield, raw counts were corrected for the decay branching ratio(BR), and for the losses due to pion/kaon in-flight decays, geometrical acceptance and detector efficiency(eff) (N_{cor} = Raw Counts/BR x eff). Absolute resonance yield in inelastic collisions is estimated using the following formula:

$$\frac{d^2N}{dp_T dy} = \frac{\text{Raw Counts}}{N_{MB} \times BR \times dp_T \times dy \times eff} \times f_{norm} \times f_{SL}$$

where N_{MB} is the number of the minimum bias trigger selected by the event cuts, BR is the branching ratio (which is the fraction of particles decaying in the desired decay mode with respect to the total number of particles decaying), eff is the acceptance x efficiency of reconstruction. The factor $f_{norm} = 0.852^{+0.062}_{-0.03}$ is efficiency for trigger selection for inelastic pp collisions. The factor $f_{SL} = 0.931264$ accounts for the signal loss introduced by the requirement that a primary vertex must be reconstructed and be in the range of ± 10 cm.

The correct value for f_{norm} for Run2 data is not yet accurately known so we use the value from Run1.

The obtained p_T spectrum for K^{*o} is shown in Figure 11.

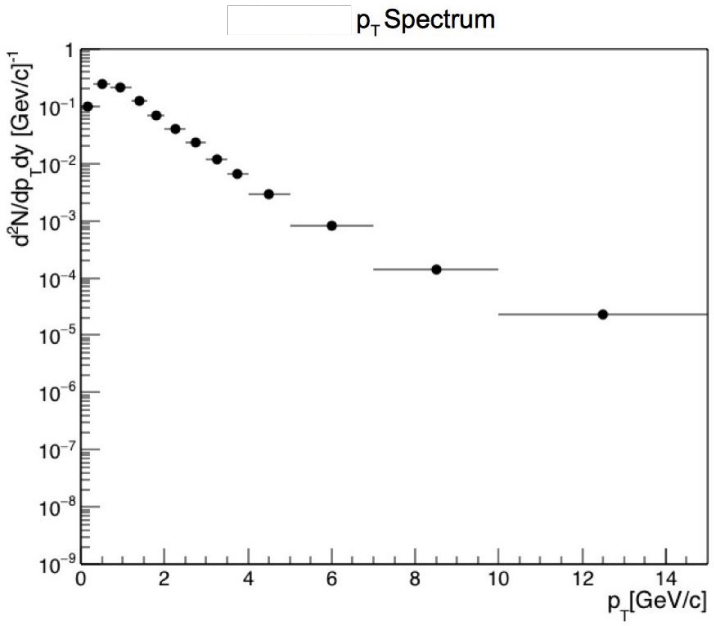

Figure 11: Transverse momentum spectrum of K^{*o} produced in pp collisions at $\sqrt{s} = 13$ TeV

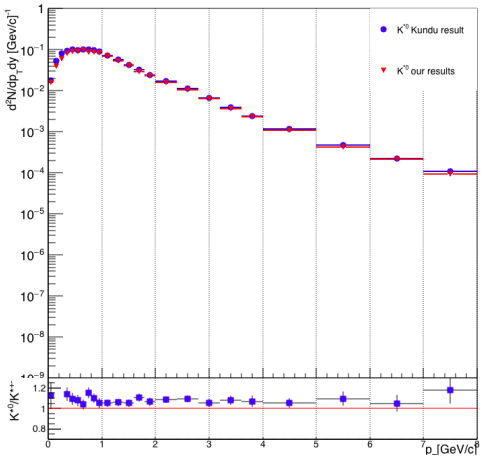

Figure 12: Spectra comparison with approved results.

Figure 12. is the comparison between the official $p_T$spectrum (blue symbols) and the ones obtained in this analysis (red symbols) . The results are divided by a factor of 2 to account for $K^{*o} + \overline{K}^{*0}$ and corrected for branching ratio and efficiency only.

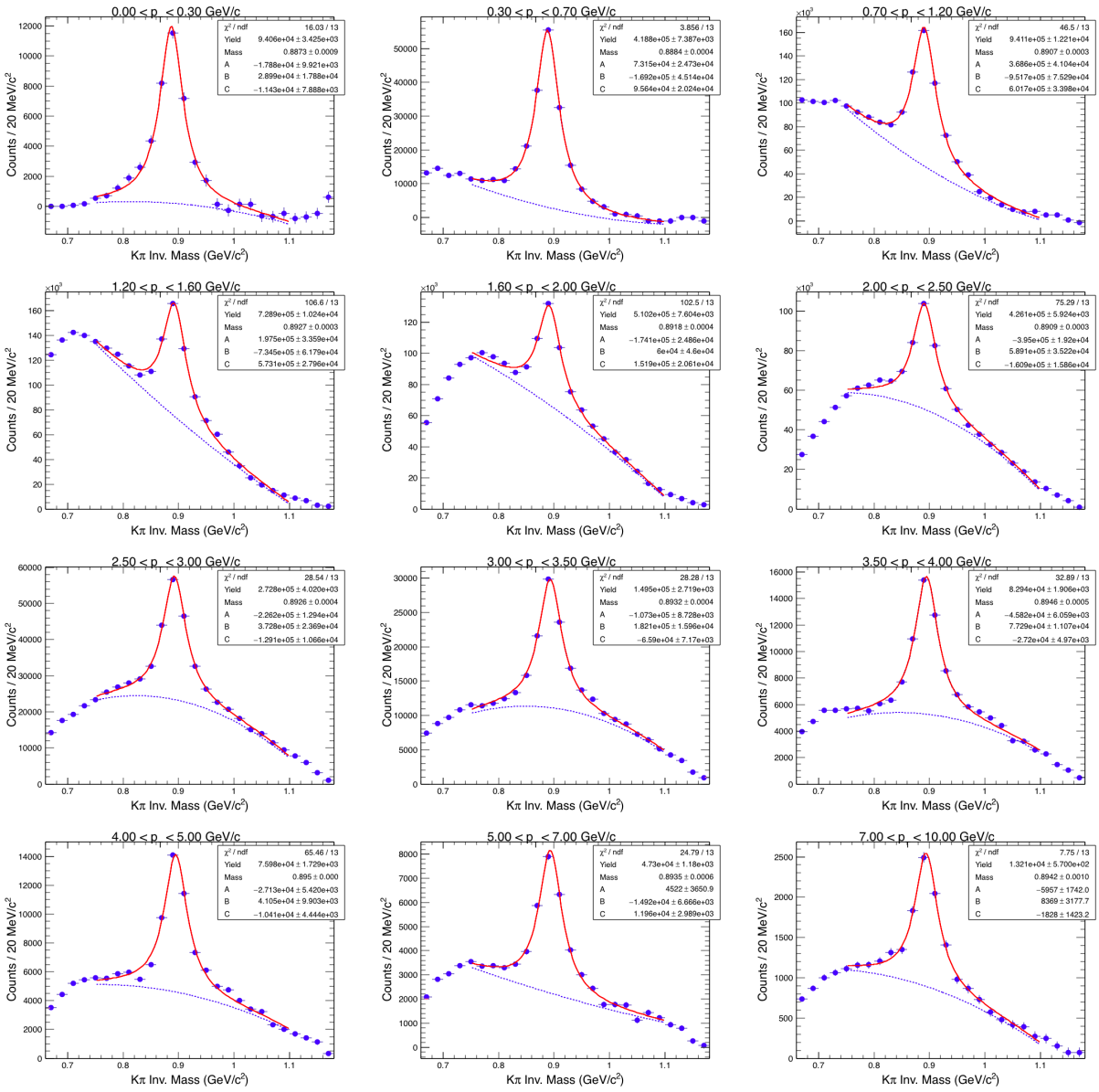

Figure 8: Fitting results from different p_T regions for BW+ Polynomial function

4 MEASUREMENT OF $K^{\pm}$ PRODUCTION IN PP COLLISIONS

$K^*(892)^{\pm}$ is a resonance particle with a small lifetime (~ 4 fm/c), comparable to that of the fireball which is produced during the heavy ion collision. Due to its short lifetime, it can be used to study the re-scattering and regeneration effects. $K^*(892)^{\pm}$ can provide the information regarding strangeness enhancement as it contains a strange quark. Measurements of $K^*(892)^{\pm}$ in pp collisions can be used as a baseline to study the Pb–Pb collisions at the LHC energy and to provide a reference for tuning event generators. This note describes the measurement of $K^*(892)^{\pm}$ mesons (in the following $K^{*\pm}$) produced at mid-rapidity ($|y| \leqslant 0.5$) in minimum-bias pp collisions at $\sqrt{s} = 13$ TeV. In this analysis, $K^{*\pm}$ has been reconstructred by its hadronic decay chanel $K^*(892)^{\pm} \rightarrow \pi^{\pm} + K^0_S$. The yield of $K^{*\pm}$ is extracted from $1K^0_S$ invariant-mass distributions as a function of transverse momentum. The p_T spectrum is integrated to obtain a measurement of the total dN/dy, and the mean transverse momentum $\langle p_T \rangle$ is extracted from the spectrum.

4.1 K^{*0} reconstruction in pp collisions

The $K^{\pm}$ production in pp collisions at $\sqrt{s} = 13$ TeV has been done with data collected in 2015 by ALICE detector. The analysis strategy is based on the invariant mass study of reconstructed pairs whose origin could be the decay of K^{*0} mesons into charged particles. The daughter particles are identified as oppositely charged pions and kaons among the tracks reconstructed in the central barrel. Track selection and particle identification is described further in this chapter. To extract the yields of K^{*0} mesons in each p_T bin, the invariant-mass distribution of unlike-charge pairs from the same event is computed. The combinatorial background is estimated by event-mixing technique and subtracted from the unlike-charge dis-

tribution. In event-mixing technique, the combinatorial background is constructed through the invariant mass of pions and kaons of different events having similar z-vertex, and multiplicity. The mixed event is normalised by the same event distribution in the region of invariant mass of 1.1 to 1.3 GeV/c^2. The signal is obtained by subtracting the mixed event combinatorial background from the same event kaon - pion invariant mass distribution. (see Figure 13)

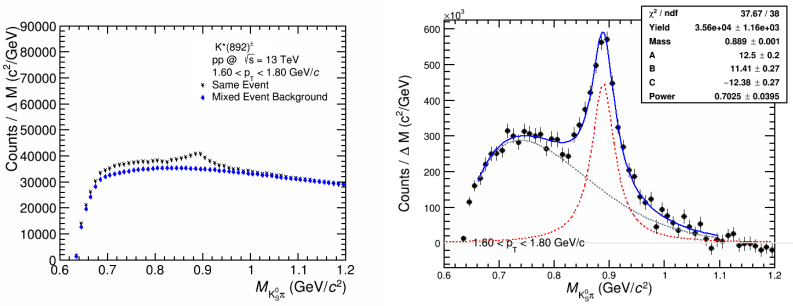

Figure 13: (Left panel) The $K^0_S\pi^\pm$ invariant mass distribution in $|y| < 0.5$ for the bin $1.6 < p_T < 1.8$ GeV/c in pp collisions at $\sqrt{s}$ = 13 TeV. The background shape estimated using pairs from different events (event-mixing technique) is shown as open green circles. (Right panel) The $K^0_S\pi^\pm$ invariant mass distribution for the bin $1.6 < p_T < 1.8$ GeV/c after background subtraction. The solid red curve is the results of the fit by eq. **??**, the dashed blue (green) curve describes the residual background (Breit-Wigner distribution).

4.2 data sample and event selection

The data used for this analysis was taken during June 2015 pp run (LHC15f, pass 2 reconstruction [1]). The full sample consists of 104 runs totalling to about 527×10^6 events. Out of these, only 48 runs have been used, which are marked by the collaboration as 'good runs' i.e. they are characterized by good performance of the detectors and good running conditions (e.g. low level of beam induced background). In particular, all these

1 A few reconstruction processes are needed to obtain data usable for physics analysis. Usually the first two reconstruction passes (pass 0 and pass 1) are needed for quality assurance check and calibration of the main detectors. The pass 2 is the first usable reconstruction for analysis purpose. Further passes are needed to implement signals from detectors requiring special calibrations.

"good runs" have both the TPC and all the ITS sub-detectors turned on.

The purpose of the event selection is to select hadronic interactions with the highest possible efficiency, while rejecting the machine-induced and physical backgrounds. The ALICE online minimum bias (MB) trigger for this pp run was configured to require the following two conditions:

(i) a signal above the threshold in VoA,

(ii) a signal above the threshold in VoC.

The threshold in the VZERO detector corresponds approximately to the energy deposition of a minimum ionizing particle.

For this analysis, a sample of 45×10^6 minimum bias pp events has been processed where ITS, TPC and TOF performance was optimal. Out of this, around 16 million events satisfy the following selection criteria and have been actually used for the analysis:

- Is InComplete DAQ check.
- Pileup Rejection using AliAnalysisUtils::IsPileUpEvent().
- SPD Clusters vs. Tracklets Check using AliAnalysisUtils::IsSPDClusterVsTrackletBC with default parameters.
- Event has a track or SPD primary vertex identified.
- SPD vertex-z resolution < 0.25 cm.
- SPD vertex dispersion < 0.04 cm.
- z-position difference between track and SPD vertex < 0.5 cm.
- vertex-z position : $|v_z| < 10$ cm.

The distribution of vertex z position of the accepted events is reported in Figure 14. Events with $|V_z| < 10$ cm have been used to ensure a uniform acceptance in the central pseudorapidity region, $|h| < 0.8$, where the analysis is performed.

4.3 $\pi^{\pm}$ and K^{o}_{S} selection

The $K^{*}(892)^{\pm}$ mesons were identified by reconstructing their decay in a charged pion ($\pi^{\pm}$) and a K^{o}_{S}. Once identified a rapidity cut ($|y| < 0.5$) has been applied to the pairs $\pi^{\pm}$ V^{o}.

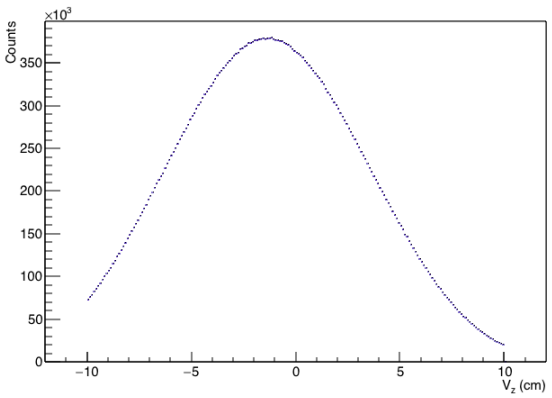

Figure 14: Vertex z coordinate distribution of the accepted events.

4.3.1 Primary pion selection

Primary charged tracks were selected by applying the following cuts:

- $p_T > 0.15$ GeV/c
- $-0.8 < \eta < 0.8$
- Reject kink daughters
- Minimum number of rows crossed in TPC is 70
- Ratio of number of crossed rows to number of findable clusters in TPC > 0.8
- Require TPC refit
- Require ITS refit
- TPC χ^2 per clusters < 4.0
- ITS χ^2 per clusters < 36.0
- χ^2 per clusters in TPC-Constrained global fit < 36.0
- Minimum number of clusters in SPD: 1 (AliESDtrackCuts::SetClusterRequirementIT kAny))
- AliESDtrackCuts::SetDCAToVertex2D(kFALSE)
- AliESDtrackCuts::SetRequireSigmaToVertex(kFALSE)
- $|DCA_z| < 2$ cm
- $DCA_r < 0.0105 + 0.0350\ p_T^{-1.1}$ (a 7σ p_T dependent cut)

These cuts, but the first two, are included in the function **AliESDtrackCuts:GetStandardITSTPCTrackCuts2011(kTRUE, 1)** which implements the standard ITS/TPC track cuts from 2011.

The primary pions were identified through their energy loss dE/dx in the Time Projection Chamber (TPC). For this analysis due to problem with TPC PID wider TPC cuts were used at low momentum. The following p-dependent PID selection cuts were applied:

- $|Nff_{TPC}| < 6$ for $p < 0.3$ GeV/c
- $|Nff_{TPC}| < 4$ for $0.3 \leqslant p \leqslant 0.4$ GeV/c
- $|Nff_{TPC}| < 3$ for $p > 0.4$ GeV/c

In Figure 15) Nff_{TPC} versus momentum p for pions without any PID cut (left panel) and after that p-dependent PID cut is applied (right panel) are shown.

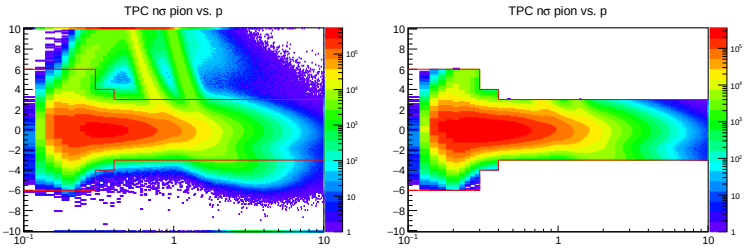

Figure 15: Nff_{TPC} versus momentum p for pions without any PID cut (left panel) and after p-dependent PID cut is applied (right panel). The dotted lines indicate the TPC PID cuts as a function of momentum.

4.3.2 V^{o} selection

The V^{o} K^{o}_{S} is identified by its decay $K^{o}_{S} \rightarrow \pi^{+} + \pi^{-}$.

The following selection criteria were applied to select the secondary pions.

Daughter track selection criteria

- $-0.8 < \eta < 0.8$
- Require TPC refit
- Reject Kink Daughters
- Minimum number of rows crossed in TPC > 70

- Ratio of number of crossed rows to number of findable clusters in TPC > 0.8
- TPC χ^2/clusters < 4.0
- DCA of tracks to PV $> 0.0105+0.0350\ p_T{}^{-1.1}$ cm (a p_T dependent cut to be complementary to primary tracks)

Furthermore secondary pions were identified through their energy loss dE/dx in the Time Projection Chamber (TPC), by a wide PID cut $|Nff_{TPC}| < 5$.

The pairs of $\pi^+\pi^-$ which fulfill the following **V^0 selection criteria** were taken as K^0_S candidates

- Only Offline V^0
- Rapidity $|y| < 2.0$
- Fiducial Volume (V^0 2D decay radius) > 0.5 cm
- V^0 cosine of pointing angle > 0.97
- DCA V^0 to Primary Vertex <0.3 cm
- DCA V^0 daughters $< 1.0\ \sigma$
- V^0 Mass Tolerance < 0.03 GeV/c^2
- Proper Lifetime (mL/p) < 20 cm

The previous cuts are the same used for the identification of K^0_S in pp collisions at $\sqrt{s}$ = 13 TeV. Only difference is for the V^0 mass cut. A V^0 mass tolerance cut was added to well select K^0_S particles. On the contrary, the competing V^0 rejection was not used since a slightly decrease of the signal without any increasing of its significance was observed. In case this rejection is used only pairs that have an invariant mass incompatible with the hypothesis to be originated from a ˜ or ˜ decay ($|M_{\tilde{}} - 1115.683| > 4$ MeV/c^2 or $|M_{\tilde{}} - 1115.683| > 4$ MeV/c^2) would be taken. Furthermore considering that we are interested only to "primary" V^0 a cut of 0.3 cm was applied on the DCA of the V^0 to the primary vertex.

5 MEASUREMENT OF $K^{\pm}$ PRODUCTION IN Pb–Pb COLLISIONS

6 FURTHER RESULTS AND DISCUSSIONS

CONCLUSIONS

In this thesis the measurement of the multi-strange baryon production in Pb–Pb and pp collisions at the centre-of-mass energy of 2.76 TeV using the ALICE apparatus have been presented. The cascade identification technique, based on the topological reconstruction of weak decays into charged particles, has been described. Such a technique is very effective thanks to the excellent particle identification and tracking capability of the ALICE central barrel detectors.